Metallodrug induced apoptotic cell death and survival attempts are characterizable by Raman spectroscopy

K. le Roux,[1] L. C. Prinsloo,[2] and D. Meyer[1,a)]
[1]Department of Biochemistry, University of Pretoria, Hatfield, Gauteng 0002, South Africa
[2]Department of Physics, University of Pretoria, Hatfield, Gauteng 0002, South Africa

(Received 7 March 2014; accepted 15 September 2014; published online 26 September 2014)

Chrysotherapeutics are under investigation as new or additional treatments for different types of cancers. In this study, gold complexes were investigated for their anticancer potential using Raman spectroscopy. The aim of the study was to determine whether Raman spectroscopy could be used for the characterization of metallodrug-induced cell death. Symptoms of cell death such as decreased peak intensities of proteins bonds and phosphodiester bonds found in deoxyribose nucleic acids were evident in the principal component analysis of the spectra. Vibrational bands around 761 cm^{-1} and 1300 cm^{-1} (tryptophan, ethanolamine group, and phosphatidylethanolamine) and 1720 cm^{-1} (ester bonds associated with phospholipids) appeared in the Raman spectra of cervical adenocarcinoma (HeLa) cells after metallodrug treatment. The significantly ($p < 0.05$, one way analysis of variance) increased intensity of phosphatidylethanolamine after metallodrug treatment could be a molecular signature of induced apoptosis since both the co-regulated phosphatidylserine and phosphatidylethanolamine are externalized during cell death. Treated cells had significantly higher levels of glucose and glycogen vibrational peaks, indicative of a survival mechanism of cancer cells under chemical stress. Cancer cells excrete chemotherapeutics to improve their chances of survival and utilize glucose to achieve this. Raman spectroscopy was able to monitor a survival strategy of cancer cells in the form of glucose uptake to alleviate chemical stress. Raman spectroscopy was invaluable in obtaining molecular information generated by biomolecules affected by anticancer metallodrug treatments and presents an alternative to less reproducible, conventional biochemical assays for cytotoxicity analyses. © *2014 AIP Publishing LLC*.
[http://dx.doi.org/10.1063/1.4896616]

Cervical cancer is the second most commonly diagnosed cancer worldwide among women, with an estimated 530 000 new cases reported annually. Every year approximately 270 000 women die of cervical cancer and >85% of recorded fatalities are found in low- and middle income countries.[1] Cervical cancer is one of the biggest health problems among South African women, affecting one out of every 41 women and mortalities associated with this disease are estimated around eight South African women per day.[2] The co-infection of human immunodeficiency virus (HIV) and human papillomavirus is well documented.[3,4] Advances in diagnoses/success of highly active antiretroviral therapy lead to HIV positive patients being diagnosed up to 10 years earlier with advanced stages of cervical cancer. With these staggering statistics in mind, new chemotherapeutic treatments are under investigation.[2]

Research into gold based compounds as potential cancer treatments started in 1980,[5] but this metal had been used centuries prior for the treatment of other ailments.[6] During the early phases of metallodrug research, it was found that derivatives containing the linear P–Au–S structure found in auranofin (a known rheumatoid arthritis drug) had potential for treating cancer.[5]

Successful cancer treatments are expected to selectively kill diseased cells only and the cytotoxic effects of the drugs are routinely monitored by conventional biochemical assays such as 3-(4,5-Dimethylthiazol-2-yl)-2,5-diphenyltetrazolium bromide (MTT) reduction assays,[7] microscopy, flow cytometric techniques,[8] and real time cell electronic sensing (RT-CES).[9] The disadvantages of some of these techniques are that expensive reagents are needed and specialised instruments to measure absorbance, impedance, fluorescence, or luminescence of labelled biosensors. An alternative to these techniques could be Raman spectroscopy where samples can be investigated in a label free manner, with minimal preparation and analyses in relatively short time periods.

In this investigation, gold (I) complexes were investigated for their cytotoxic effect on a cancer cell line. We suggest Raman spectroscopy as a practical tool for the characterization of chemically induced cell death in a population.

Two organic gold complexes 2-(2-(diphenylphosphino) ethyl)pyridyl-gold(I) chloride (AE 76) and 2-(diphenyl phosphino)-2′-(N,N-dimethylamino)biphenylgold(I) chloride (AE125) were synthesized and characterized[35,36] by the laboratory of Professor Darkwa in the Chemistry Department of the University of Johannesburg, South Africa. Details of the synthesis and characterization can be found in the Ph.D. thesis of Elkhadir, 2014.[37] Auranofin (Sigma, Germany) was used as a positive control drug for the induction of apoptosis.[10,11]

Apoptotic cell death induction by the metallodrugs was determined using flow cytometry. Exponentially growing HeLa cells were seeded (10^5 cells/ml) and incubated for 24 h (37 °C, 5% CO_2) after which the cells were exposed to the metallodrugs (auranofin = 5.6 μM, AE76 = 20.8 μM, and AE125 = 17.8 μM) for 72 h. After treatment, detached cells were collected and the

a)Author to whom correspondence should be addressed. Electronic mail: debra.meyer@up.ac.za. Tel.: +2712 420 3200. Fax: +2712 362 5302.

wells washed with 500 μl phosphate buffered saline (PBS). The cells were rinsed with 200 μl trypsin (Hyclone) and incubated for 5 min. Trypsinized cells were washed twice with the respective collected media, thus pooling detached and adherent cells. Pooling cells was capable in this case because the cells were in various stages of cell death. Samples were prepared for annexin-V and propidium iodide staining as prescribed by the manufactures (BD Biosciences, California, USA) and analysed using a fluorescence-activated cell sorter (FACS) Aria. Four independent experiments were performed and expressed as % cell events with standard error of the mean. Data were analysed statistically using one way analysis of variance (ANOVA) where $p < 0.05$ was documented as significant.

After the quantification of apoptosis (with flow cytometry), a qualitative Raman spectroscopic study was done to determine the molecular changes. The method published by Matthaus *et al.*[12] was used as a guideline. Cells were prepared in the same manner as for flow cytometry and pooling cells which were centrifuged for 10 min at 1200 reps per minute. The supernatant was discarded, the pellets loosened, and the cells washed twice with 1 ml PBS. The cells were incubated at room temperature in 1 ml of 10% formalin for 10 min and then centrifuged for 5 min. The cells were washed with 1 ml sterile distilled water and centrifuged to remove all traces of formalin. The cells were suspended in 10 μl sterile distilled water. Three microliters cell suspension was dried in the biosafety flow hood for 1 h on sterile CaF_2 discs. Raman microspectroscopy was performed with a T64000 micro-Raman spectrometer from HORIBA Scientific. The 514.5 nm line of an Innova 70v argon-krypton mixed gas laser was used as excitation source. The 50× objective of an Olympus microscope was used to focus the laser beam (spot size $\sim 2\,\mu$m) in the middle of single air-dried cells, where the nuclei is most likely situated as is the norm.[13–16] The laser power at the sample was kept constant at 10 mW. Three independent experiments were carried out of which a total of seven cells per treatment were analysed. All the spectra were recorded with a 150 s acquisition time for two accumulations. The Labspec 6.0 software was used to fit and subtract a fourth order polynomial function to obtain a zero baseline. A 5 degree linear Savitsky-Golay smoothing procedure was applied to all the spectra. Second derivatives of the spectra (vector normalized) were used for final interpretations (generated in OPUS 7). Principal component analysis (PCA) was carried out using Quant 2 OPUS software. Vibrational peaks of interest involving phospholipid and glucose metabolism were validated with one way ANOVA followed by Tukey's multiple comparison test using GraphPad Prism 5. Changes in vibrational peaks were significant if $p < 0.05$.

The metallodrugs were evaluated using conventional biochemical methodologies to determine the degree of cytotoxicity and the type of cell death induction. Raman spectroscopy was then used to identify molecular targets of the metallodrugs and the drug induced effects on phospholipid and glucose metabolism. Flow cytometric analysis detected that early apoptosis was significantly ($p < 0.05$) induced by the metallodrugs (Fig. 1).[11] Less than 14% of the cells was viable, confirming light microscopic evidence which indicated that all cells treated with AE 76 and auranofin experienced severe chemical distress after treatment.

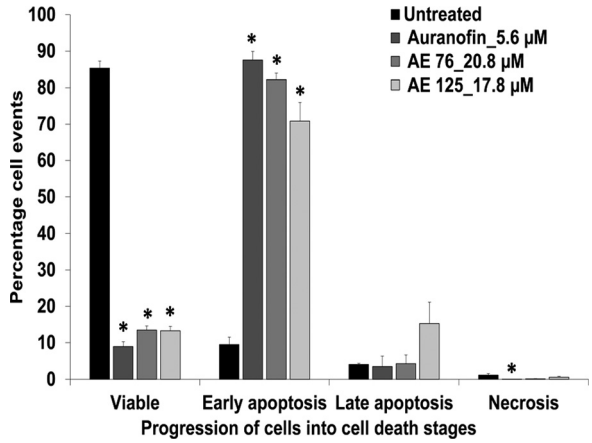

FIG. 1. Flow cytometry: The percentages viable and dead HeLa cells after treatment with different concentrations of metallodrugs. The induction of early apoptosis was significant (*$p < 0.05$) for all treatments. Necrotic events were negligible and late apoptosis was minimal ($n = 4$).

Further insight into the mechanism of action of the three metallodrugs was determined by studying the molecular vibrations of the chemically stressed cells. The investigation was focused on the centre of the HeLa cells. This area of cells are known to be rich in nuclear material such as proteins, lipids, nucleic acids, nuclear membranes, and plasma membranes.[13,15,17] The hallmarks of apoptosis involve the nucleus (chromatin condensation and deoxyribose nucleic acids (DNA) fragmentation, etc.[18]) and are well documented. The raw spectra of the cells analysed in this study[11] had vibrational peaks for proteins, lipids, nucleic acids, and carbohydrates and were comparable to previously reported spectra obtained for HeLa cells including Raman spectra of the nucleus.[12,16] Since only small variances were seen in the raw spectra of untreated and metallodrug treated spectra, second derivatives were used for further discussion (Fig. 2). The most prominent peaks in the spectra belonged to protein vibrations, namely, methyl (CH_3) stretch vibrations (2927 cm^{-1}), amide I at 1657 cm^{-1} (overlapping with peaks originating from fatty acids including triglycerides), amide III overlapping with asymmetric phosphate stretching modes (1224 cm^{-1}), phenylalanine (1006 cm^{-1}), and tyrosine (1165 cm^{-1}).[19] The intensity of CH_2 symmetric stretch vibrations (2862 cm^{-1}) of lipids/proteins[19] and carbon-hydrogen (CH) and CH_2 vibrations[19] at 1449 cm^{-1} were also prominent. Cellular responses to treatment were heterogeneous, probably due to different degrees of sensitivity[20] of individual cells to the treatments. Heterogeneity of the spectra could also be due to the spectra only being recorded for the centre of the cell, where nuclear material could be showing different stages of apoptotic progression (chromatin condensation would be presented by increased DNA intensities compared to decreased DNA intensities due to DNA fragmentation[21,22]). The cell number was sufficient for this study,[15,21,23,24] since it was qualitative and was carried out on well-defined populations of viable and apoptotic cells as determined with flow cytometry.

Focusing on single peaks is not sufficient when describing the major peak shifts seen in this study which is why PCA was used for further analysis.[13] Cells were not deliberately synchronized but our data (Fig. 3) showed that

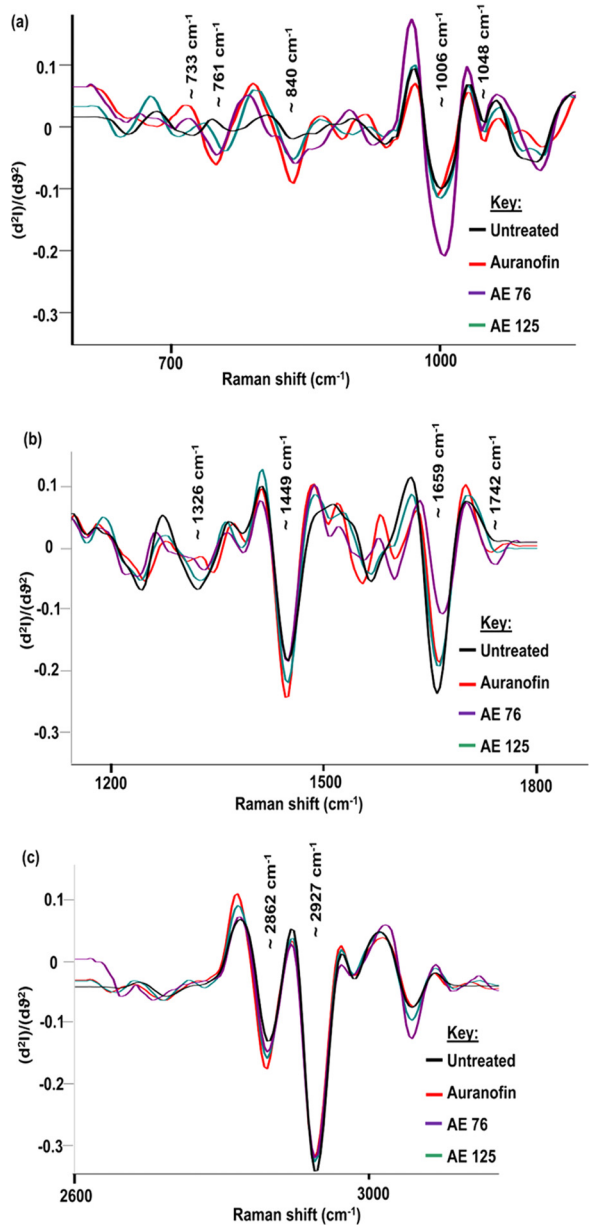

FIG. 2. The second derivatives of untreated and metallodrug treated HeLa cells in the regions between (a) 600–1150 cm^{-1}, (b) 1150 cm^{-1}–1800 cm^{-1}, and (c) 2600–3200 cm^{-1}. Major spectral differences are visible which indicate aspects of the mechanism of action of these metallodrugs and also induction of apoptotic cell death.

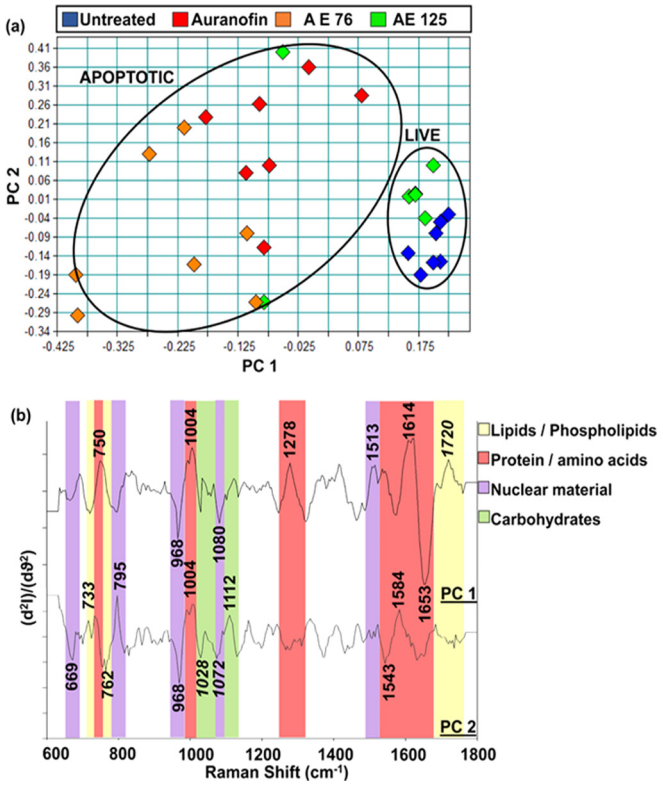

FIG. 3. Principal component analysis score plots comparing the second derivatives of the Raman spectra of (a) the region of 600–1800 cm^{-1}, "live" and less damaged cells, while all others clustered together (dead) and (b) corresponding loading spectra leading to the clustering in the PCA plot. Assigned components were identified as major contributors of separation.

intercellular variations was low. The occurrence can be explained by the study of Matthews *et al.*[25] where cells were mostly in one (gap 1) phase. Score plots were used to identify significant changes between untreated and treated HeLa cells. It was found that most of the spectral variance was within the first PC between the 600–1800 cm^{-1} region. In the case of PC 1, the untreated cells clustered separately from the treated cells, with the exception of some of the spectra of AE 125 treated cells (Fig. 3(a)). This clustering is explained by the different stages of cellular responses after treatment. Although all cells were exposed to AE 125 simultaneously, the exact amount absorbed may differ so that individual cells are at different stages of early apoptosis allowing some to behave as if unaffected by treatment (as if untreated), while others present a more severe response. Flow cytometry showed a population of seemingly healthy cells migrating towards early apoptosis after cells were treated with AE 125.[11] These trends in cellular responses were also prominent in the study conducted by Brauchle *et al.*, which found that Saos-2 and SW-1353 apoptotic cells (exposure to room temperature for 4 days) also showed poor separation on PCA score plots.[13] In the AE 76 treated cells, the spectra showed a higher degree of spectral variance between samples, but all cells behaved as if apoptotic. The differences in response between treatments are explained by their structural differences. The many bulky aromatic rings of AE 125 certainly affect its cellular absorption.

Clustering of untreated and treated HeLa cells showed strong separation along PC 1. Spectra obtained from metallodrug treated cells were associated with negative scores in the score plot. Since the PCA was performed on second derivatives, a negative score was associated with a positive loading.[26] The positive loadings in PC 1 corresponded to a decrease in tryptophan (750 cm^{-1}), phenylalanine (1004 cm^{-1}), amide III (1275 cm^{-1}), cytosine (1513 cm^{-1}), and a combination of tyrosine, tryptophan, and C=C protein vibrations (1614 cm^{-1})[19] and was associated with treated HeLa cells. The positive loadings were packed with amino acid, and protein vibrations decreased as compared to untreated HeLa cells. The negative loadings in PC 1 corresponded to lipid vibration (968 cm^{-1}), phospholipids and phosphodiester groups of nucleic acids (1080 cm^{-1}), and C=C, carbonyl (C=O) (lipids), and amide I (1653 cm^{-1})[19] (Fig 3(b)). The negative loadings were associated with untreated and some AE125 cells therefore indicative

of the other treated cells having lower intensities in some proteins, phospholipids, and other lipids as well as phosphodiester groups associated with nucleic acids as compared to viable cells. These findings were in agreement with other researchers.[15,21,27] PC 1 explained the highest variance within the spectra, while some clustering could be seen due to PC 2 loadings. Negative loadings of PC 2 corresponded to cytosine ($669\,cm^{-1}$), phosphatidylethanolamine ($761\,cm^{-1}$), lipids ($968\,cm^{-1}$), and amide II ($1543\,cm^{-1}$).[19] Positive loadings of PC 2 were DNA ($795\,cm^{-1}$), phenylalanine ($1004\,cm^{-1}$), carbohydrates ($1112\,cm^{-1}$), and phenylalanine ($1586\,cm^{-1}$). The decrease of a band at $795\,cm^{-1}$ had been suggested by previous researchers to be related to internucleosomal DNA cleavage.[13,15,20] Negative loadings of PC 2 were associated with the increase in glucose ($1072\,cm^{-1}$) and glycogen ($1028\,cm^{-1}$), indicating noteworthy changes in the metabolism of treated cells, which were further investigated to determine the significance of the metabolites.

Changes in carbohydrate vibrational peaks could give more insight into the metabolic functions of the treated cells. Peaks assigned to glycogen was identified in the PCA loadings around $853\,cm^{-1}$, $918\,cm^{-1}$, $935\,cm^{-1}$, $1028\,cm^{-1}$, $1155\,cm^{-1}$, and $1335\,cm^{-1}$.[19,27–29] The bands at $1028\,cm^{-1}$ and $1155\,cm^{-1}$ significantly ($p < 0.05$)[11] increased in intensity. Together with the peak at $1072\,cm^{-1}$ identified in the PCA, other glucose and polysaccharides related peaks, $898\,cm^{-1}$ and $920\,cm^{-1}$, were also identified.[19] The peak at $1072\,cm^{-1}$ significantly increased. Changes in the intensities of glycogen or glucose could be indicative of a survival mechanism of chemically stressed cancer cells. Higher concentrations of glucose within the cells could be due to the active up take of glucose from the nutrient rich culture media, while the surplus glucose within the cells were stored as glycogen. Although the apoptotic process had already started as detected with flow cytometry and Raman spectroscopy, it is generally known that cancer cells do not die easily and thus will try to excrete any of the drugs taken up. Energy to sustain the excretion of the metallodrugs could come from glucose.

In the PCA, loading plots indicated spectral changes in phospholipids. Spectral peaks associated with the plasma membrane were identified and further analysed to determine significant changes which could be linked to flow cytometry results. The laser pathway through the cell interrogates the plasma membrane, cytoplasm, nuclear membranes, and nuclear material. The peaks at $733\,cm^{-1}$ and $787\,cm^{-1}$ in spectra of the untreated cells were assigned to phosphatidylserine.[19,30] Phosphatidylserine forms part of the inner leaflet of the plasma membrane and make up 2%–10% of all the phospholipids found in the plasma membrane.[31] During apoptosis, a conformational change takes place within the bilayer of the plasma membrane. This conformational change occurs when phosphatidylserine is externalized on the cellular surface. It was found that the peaks changed significantly[11] in intensity after treatment. Phosphatidylethanolamine ($761\,cm^{-1}$ and $1300\,cm^{-1}$)[19,30] is also located in healthy cells on the inner leaflet of the plasma membrane and forms between 20% and 50% of the membrane composition.[31] This peak was evident after the HeLa cells were treated with auranofin and AE76 (Fig. 2). Phosphatidylethanolamine is co-regulated with phosphatidylserine and externalized during apoptosis.[32,33] This existing relationship between these two phospholipids could potentially be used for the detection of apoptosis using Raman spectroscopy. The band at $1720\,cm^{-1}$ was assigned to carbonyl and ester groups associated with phospholipids,[19] an increase in phospholipids could be due to the formation of lipid rich vesicles which forms during apoptosis.[22] The decrease in the peak at $733\,cm^{-1}$ together with the prominent appearance of the peak at $761\,cm^{-1}$ and significant increase in $1720\,cm^{-1}$ appear to be indicative of induced apoptosis.

To summarize; the interpretations of Raman spectroscopy data allowed for a detailed description of the mechanism of action of the metallodrugs tested (some metallodrugs were superior at inducing apoptosis quicker). Changes in vibrational bands assigned to phosphatidylethanolamine were indicative of apoptosis. Confirmatory experiments using other methodologies are needed to validate this finding, e.g., the detection of fluorescent anti-phosphatidylethanolamine antibodies using enzyme-linked immunosorbent assay, fluorescent microscopy, or flow cytometry.[32,34] Correlations between flow cytometric data and Raman spectra was evident in the detection of indicators of apoptosis. The increase of glucose peak intensities was also unmistakable and knowing the important role that this metabolite plays during cancer cell survival (high levels of glucose consumption involved in excreting chemotherapy) supports this observation.

The authors would like to acknowledge the following organizations for funding this project: the University of Pretoria, the Technology Innovation Agency (TIA), and the National Research Foundation (NRF) of South Africa.

[1]W. H. Organisation, Fact Sheet No. 380, 2013.
[2]L. C. Snyman, S. Afr. J. Obstet. Gynaecol. **19**, 2 (2012).
[3]Z. M. Chirenje, Best Pract. Res. Clin. Obstet. Gynaecol. **19**, 269 (2005).
[4]A. Amit, C. L. Edwards, P. Athey, and A. L. Kaplan, Int. J. Gynecol. Cancer **11**, 78 (2001).
[5]E. R. T. Tiekink, Inflammopharmacology **16**, 138 (2008).
[6]V. Milacic, D. Fregona, and Q. P. Dou, Histol. Histopathol. **23**, 101 (2008).
[7]C. Wetzel, P. C. Kunz, M. U. Kassack, A. Hamacher, P. Böhler, W. Watjen, I. Ott, R. Rubbiani, and B. Spingler, Dalton Trans. **40**, 9212 (2011).
[8]C.-M. Che, R. W.-Y. Sun, W.-Y. Yu, C.-B. Ko, N. Zhu, and H. Sun, Chem. Commun. **2003**(14), 1718.
[9]P. N. Fonteh, F. K. Keter, and D. Meyer, J. Inorg. Biochem. **105**, 1173 (2011).
[10]A. B. Mullick, Y. M. Chang, I. Ghiviriga, K. A. Abboud, W. Tan, and A. S. Veige, Dalton Trans. **42**, 7440 (2013).
[11]See supplementary material at http://dx.doi.org/10.1063/1.4896616 for details on the metallodrugs, flow cytometry zebra plots, raw Raman data, one way ANOVA, and Tukey multiple comparison test.
[12]C. Matthaus, T. Chernenko, J. A. Newmark, C. M. Warner, and M. Diem, Biophys. J. **93**, 668 (2007).
[13]E. Brauchle, S. Thude, S. Y. Brucker, and K. Schenke-Layland, Sci. Rep. **4**, 4698 (2014).
[14]A. Fujioka, K. Terai, R. E. Itoh, K. Aoki, T. Nakamura, S. Kuroda, E. Nishida, and M. Matsuda, J. Biol. Chem. **281**, 8917 (2006).
[15]S. Verrier, I. Notingher, J. M. Polak, and L. L. Hench, Biopolymers **74**, 157 (2004).
[16]C. Matthaus, S. Boydston-White, M. Miljkovic, M. Romeo, and M. Diem, Appl. Spectrosc. **60**, 1 (2006).
[17]G. Perna, M. Lasalvia, P. D'Antonio, N. L'Abbate, and V. Capozzi, J. Raman Spectrosc. **42**, 603 (2011).
[18]S. Elmore, Toxicol. Pathol. **35**, 495 (2007).
[19]Z. Movasaghi, S. Rehman, and I. U. Rehman, Appl. Spectrosc. Rev. **42**, 493 (2007).

[20]T. J. Moritz, D. S. Taylor, D. M. Krol, J. Fritch, and J. W. Chan, Biomed. Opt. Express **1**, 1138 (2010).
[21]I. Notingher, S. Verrier, S. Haque, J. Polak, and L. Hench, Biopolymers **72**, 230 (2003).
[22]I. Martin, V. I. Poon, Z. Petropoulos, S. Harder, and J. Lum, J. Cancer Res. Ther. Oncol. **1**, 1 (2013).
[23]A. Zoladek, F. Pascut, P. Patel, and I. Notingher, J. Raman Spectrosc. **42**, 251 (2011).
[24]I. Notingher, J. Selvakumaran, and L. L. Hench, Biosens. Bioelectron. **20**, 780 (2004).
[25]Q. Matthews, A. Jirasek, J. Lum, X. Duan, and A. G. Brolo, Appl. Spectrosc. **64**, 871 (2010).
[26]K. L. Munro, K. R. Bambery, E. A. Carter, L. Puskar, M. J. Tobin, B. R. Wood, and C. T. Dillon, Vib. Spectrosc. **53**, 39 (2010).
[27]H. Yao, Z. Tao, M. Ai, L. Peng, G. Wang, B. He, and Y. Li, Vib. Spectrosc. **50**, 193 (2009).
[28]C. M. Krishna, G. D. Sockalingum, R. A. Bhat, L. Venteo, P. Kushtagi, M. Pluot, and M. Manfait, Anal. Bioanal. Chem. **387**, 1649 (2007).
[29]A. Salman, E. Shufan, L. Zeiri, and M. Huleihel, Biochim. Biophys. Acta **1830**, 2720 (2013).
[30]C. Krafft, L. Neudert, T. Simat, and R. Salzer, Spectrochim. Acta Part A **61**, 1529 (2005).
[31]R. Chaurio, C. Janko, L. E. Munoz, B. Frey, M. Herrmann, and U. S. Gaipl, Molecules **14**, 4892 (2009).
[32]J. H. Stafford and P. E. Thorpe, Neoplasia **13**, 299 (2011).
[33]K. Emoto, N. Toyama-Sorimachi, H. Karasuyama, K. Inoue, and M. Umeda, Exp. Cell Res. **232**, 430 (1997).
[34]M. Sanmarco and M.-C. Boffa, Lupus **18**, 920 (2009).
[35]N. W. Alcock, P. Moore, P. A. Lampe, and K. F. Mok Dalton Trans. **1982**, 207 (1982).
[36]M. J. Calhorda, C. Ceamanos, O. Crespo, M. C. Gimeno, A. Laguna, C. Larraz, P. D. Vaz, and M. D. Villacampa, Inorg. Chem. **49**, 8255 (2010).
[37]A. Y. F. Elkhadir, "Phosphorous-nitrogen gold (I), palladium (II) and platinum (II) bimetallic complexes as potential antimalaria, antiHIV, antimycobateria, and anticancer agents," Ph.D. thesis (University of Johannesburg, 2014).